

SUPPLEMENTARY FIGURE LEGENDS

Figure S1. **Morphology of MEF WT and p27 KO in 2D- and 3D-cultures.** (A) Phase contrast microscopy of MEF WT or p27 KO exponentially growing in a culture dish. A typical image is shown, using a 10x objective. (B) Phase contrast microscopy of MEF WT or p27 KO included in 3D-Collagen I in complete medium (CM), for the indicated times. Typical images are shown, using a 20x objective. (C) Phase contrast microscopy of MEF WT or p27 KO included in 3D-Collagen I in serum free medium (SFM), for the indicated times. Typical images are shown, using a 20x objective.

Figure S2. **Characterization of stable cell clones expressing the empty vector.** (A) Western Blot analysis of p27, stathmin and vinculin (used as loading control) in 3T3 fibroblasts WT (left panel) or p27 KO (right panel) transduced with MSCV empty vectors. MW markers are indicated on the right. (B) Phase contrast microscopy of 3T3 fibroblasts WT or p27 KO control cells or transduced with MSCV empty vectors, exponentially growing in a culture dish (upper panels), included in 3D-Matrigel (middle panels) or in 3D-Collagen I (lower panels). Typical images are shown, using a 20x objective. (C) Matrigel evasion assay of 3T3 fibroblasts WT or p27 KO control cells or transduced with MSCV empty vectors. Dashed line highlights the Matrigel drop edge. Typical images are shown at 4 days from cell inclusion, using a 10x objective. (D) Same as in (C) but after 10 days of inclusion and following crystal violet staining of the drops. (E) Wound healing assay of 3T3 fibroblasts WT or p27 KO control cells or transduced with MSCV empty vectors. Typical images are shown at Time 0 and at 24 hours from scratch, using a 10x objective. Dashed line highlights the scratch margin.

Figure S3. **Stathmin is responsible for the rounded morphology of p27 KO fibroblasts.** (A) Bright field microscopy of 3T3-fibroblasts WT, p27 KO or p27 KO stably re-expressing p27, included in 3D-Collagen I for 6 hours. A 10x objective was used. (B) Cells in (A) have been classified by microscope observation in three morphological categories, i.e. round, elongated (two opposed protrusions) or stellate (>2 protrusions), and data regarding this analysis are reported in the graph, that represents the mean of 3 independent experiments in which the cells present in at least 5 randomly selected fields have been counted. (C) Same as in (A) but regarding 3T3-fibroblasts WT, p27 KO and stable cell clones over-expressing Stathmin in both genetic backgrounds. (D) Same as in (B), regarding the experiment described in (C). (E) Single cell speed of 3T3-fibroblasts WT, p27 KO and stable cell clones over-expressing Stathmin included in 3D-Collagen I, calculated using time lapse video microscopy coupled with a semi-automatic cell tracking software. Data represent the mean of three independent experiments in which 40 cells for each cell line were tracked (Mann-

Whitman U-Test). (F) Same as in (E) but regarding 3T3-fibroblasts WT, p27 KO or p27 KO stably re-expressing p27. Data represent the mean of three independent experiments in which 40 cells for each cell line were tracked (Mann-Whitman U-Test).

Figure S4. **Characterization of stable cell clones overexpressing stathmin.** (A) Western Blot analysis of p27, stathmin and vinculin (used as loading control) in 3T3 fibroblasts WT (left panel) or p27 KO (right panel) transduced with empty vector or a vector expressing stathmin. MW markers are indicated on the right. (B) Phase contrast microscopy of 3T3 fibroblasts WT or p27 KO expressing the MSCV empty vectors or stathmin, exponentially growing in a culture dish. Typical images are shown, using a 20x objective. (C) Wound healing assay of 3T3 fibroblasts WT or p27 KO transduced with empty vector or a vector expressing stathmin. Typical images are shown at Time 0 (upper panels) and at 24 hours (lower panels) from scratch, using a 10x objective. Dashed line highlights the scratch margin. (D) MTT proliferation assay on 3T3 fibroblasts WT or p27 KO transduced with empty vector or a vector expressing stathmin. (E) FACS analysis of cell cycle distribution of 3T3 fibroblasts WT or p27 KO transduced with empty vector or a vector expressing stathmin, harvested at high confluence conditions. (F) Western Blot analysis of indicated cell cycle proteins in 3T3 fibroblasts WT or p27 KO transduced with empty vector or a vector expressing stathmin, harvested following serum starvation overnight and release in complete medium for the indicated times. MW markers are indicated on the right.

Figure S5. **Morphological and motile behavior of stathmin clones.** (A) Phase contrast microscopy of 3T3 fibroblasts WT or p27 KO expressing the MSCV empty vectors or stathmin, included in 3D-Matrigel. Typical images are shown at 3 hours from inclusion, using a 20x objective. (B) Matrigel evasion assay of 3T3 fibroblasts WT or p27 KO expressing the MSCV empty vectors or stathmin. Dashed line highlights the Matrigel drop edge. Typical images are shown at 4 days from cell inclusion, using a 10x objective. (C) Haptotaxis to Collagen I or Fibronectin-coated transwells of 3T3 fibroblasts WT, p27 KO or WT overexpressing stathmin, seeded in the top chamber of the insert. Migrated cells after 12 hours are reported as fold induction over the WT cells. Data are the mean of two independent experiments performed in duplicate.

Figure S6. **Generation of p27/Stathmin double knock-out (DKO) fibroblasts.** (A) PCR analysis on genomic DNA extracted from different MEF populations. Specific primers to identify the WT and KO allele of p27 and stathmin were used. (B) Phase contrast microscopy of MEF WT, p27 KO and two DKO exponentially growing in a culture dish (upper panels) or included in 3D-Collagen I, in complete medium (CM, middle panels) or in serum free medium (SFM, bottom panels). A typical image is shown, using a 10x objective. (C) Wound healing assay on MEF WT, p27 KO and DKO. The graph reports the percentage of wound closure after 4 and 8 hours of incubation respect

to the time zero for each genotype. Results represent the mean of three experiments, performed in duplicate. The differences among genotypes were not statistically significant. **(D)** Haptotaxis to Collagen I-coated transwells of MEF WT, p27 KO and DKO, seeded in the top chamber of the insert. Migrated cells at the indicated time points are reported in the graph as percentage of total cell number. Results represent the mean of three independent experiments performed in duplicate. **(E)** Collagen evasion assay. MEF WT, p27 KO and DKO have been included in Collagen I drops and monitored over the time. A typical image is shown, taken 24 hours from cell inclusion using a 10x objective. The dashed line underlines the drop edge.

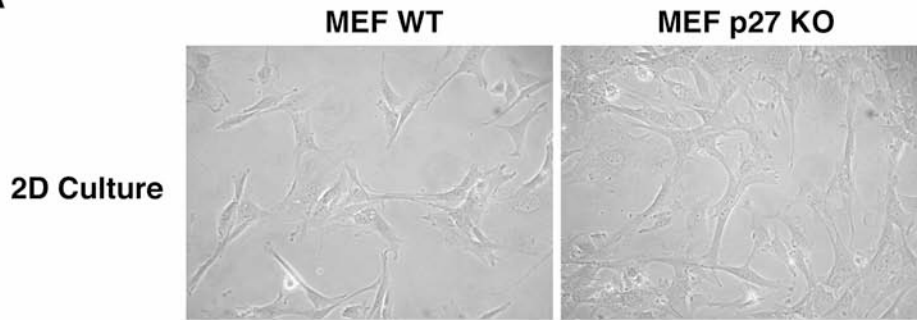
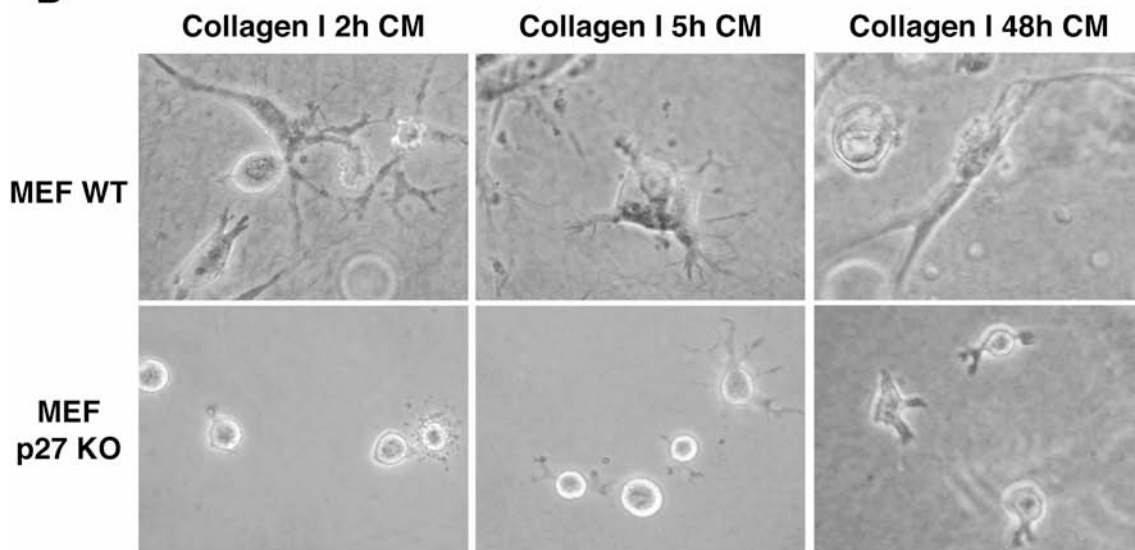
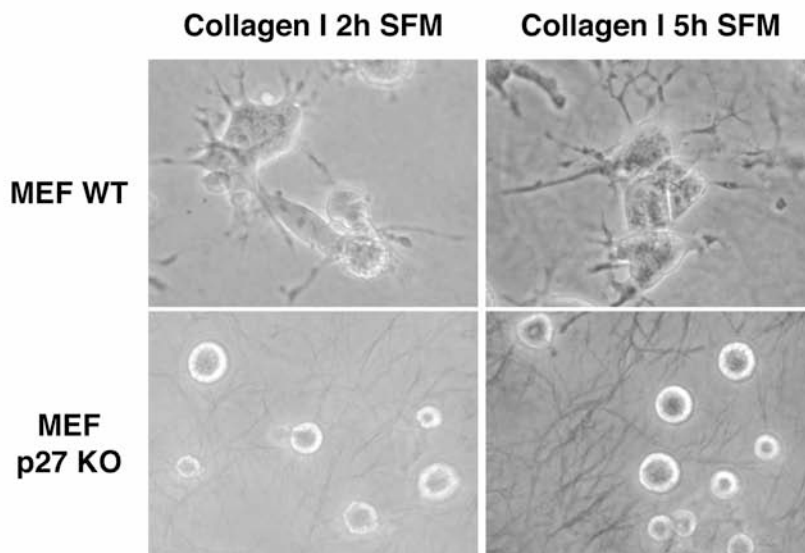
Figure S7. **MT stability of DKO fibroblasts is comparable to that of WT cells.** **(A)** Quantitative adhesion assay (CAFCA, see materials and methods section) of MEF WT, p27 KO and DKO on the indicated ECM substrates. Bovine serum albumin (BSA) was used as negative control. Results are expressed as percentage of adhered cells over the total, and represent the mean of three different experiment performed in sextuplicate. **(B)** Western Blot analysis of soluble and polymerized protein fractions from MEF WT, p27 KO and DKO adhered to Fibronectin (FN) for 1 hour. Quantification of the percentage of acetylated tubulin present in the polymerized fraction respect to the total amount is reported in the graph on the right. **c.** Western Blot analysis of soluble and polymerized protein fractions from 3T3 fibroblasts WT, p27 KO and DKO adhered to Fibronectin (FN) for 30 and 60 minutes. Quantification of the percentage of acetylated- and de-tyrosinated-tubulin present in the polymerized fraction respect to the total amount is reported in the graphs on the right.

Figure S8. **Rounded cell morphology of p27 KO cells in 3D relies on high RhoA activity.** **(A)** Phase contrast microscopy of MEF WT, p27 KO and DKO, included in 3D Collagen I (control) in the presence of Y27632 10 μ M or C3 exoenzyme 2 μ g/ml. Typical images are shown, using a 20x objective. **(B)** Phase contrast microscopy of WT, p27 KO and p27 KO fibroblasts treated with Y27632 10 μ M included in 3D-Matrigel. Typical images are shown, using a 20x objective. **(C)** Immunofluorescence analysis of RhoA (AF488, green), F-Actin (Phalloidin, AF647, pseudocolored in blue) and lipid rafts (CTxB AF594, red) in MEF WT, p27 KO and DKO. Cells were labeled with CTxB, detached, kept in suspension for 30 minutes, adhered to FN-coated coverslips for 30' and then fixed. Yellow arrows indicate membrane localization of CTxB and Rho. Typical images are shown, using a 60x objective.

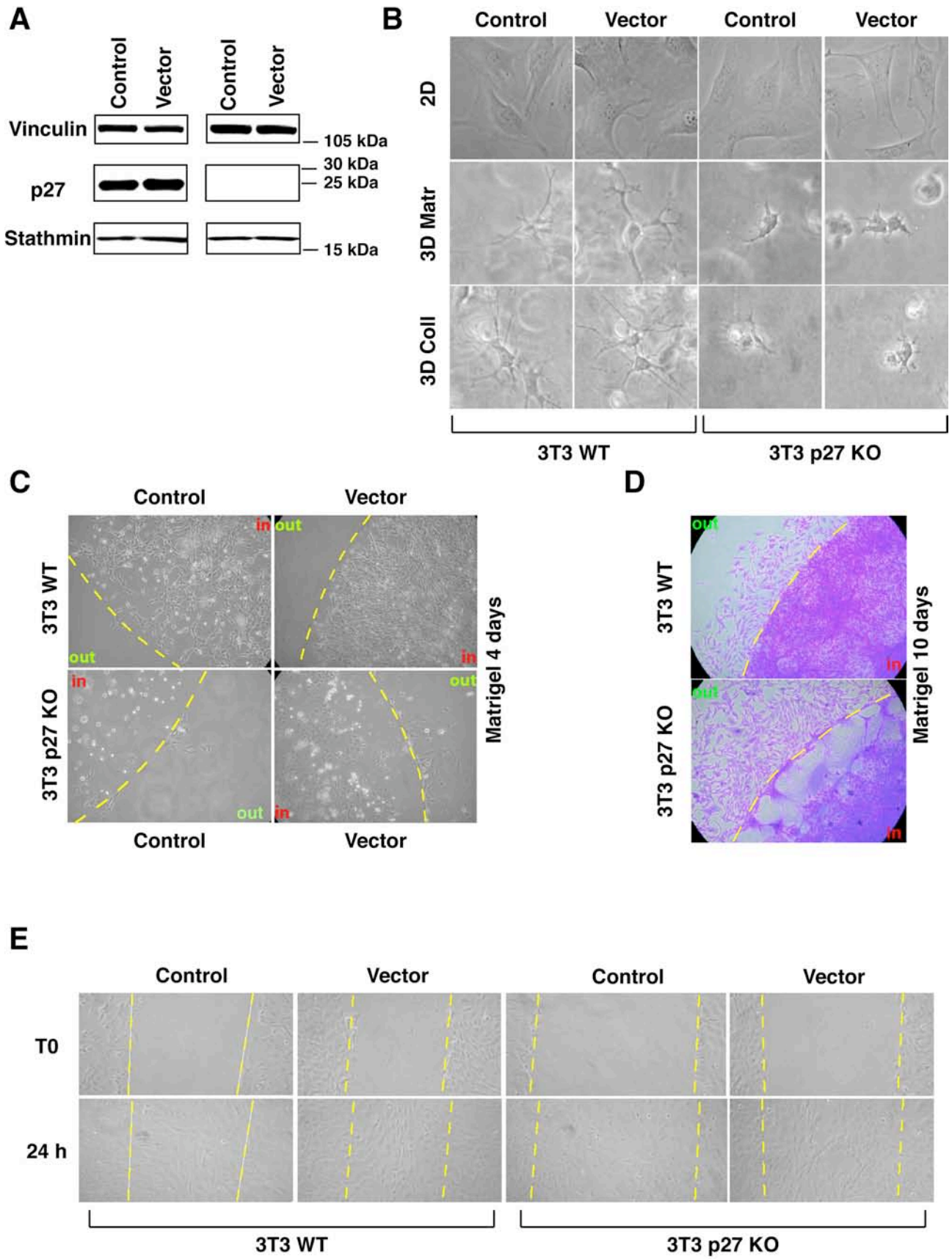
SUPPLEMENTARY VIDEO LEGENDS

Video S1 shows that WT cells immersed in 3D-Collagen I start to form protrusion within 2 hours from inclusion. **Video S2** shows that Cytochalasin D retarded but did not abolish protrusion formation in WT cells immersed in 3D-Collagen I. **Video S3** shows that treatment with low doses

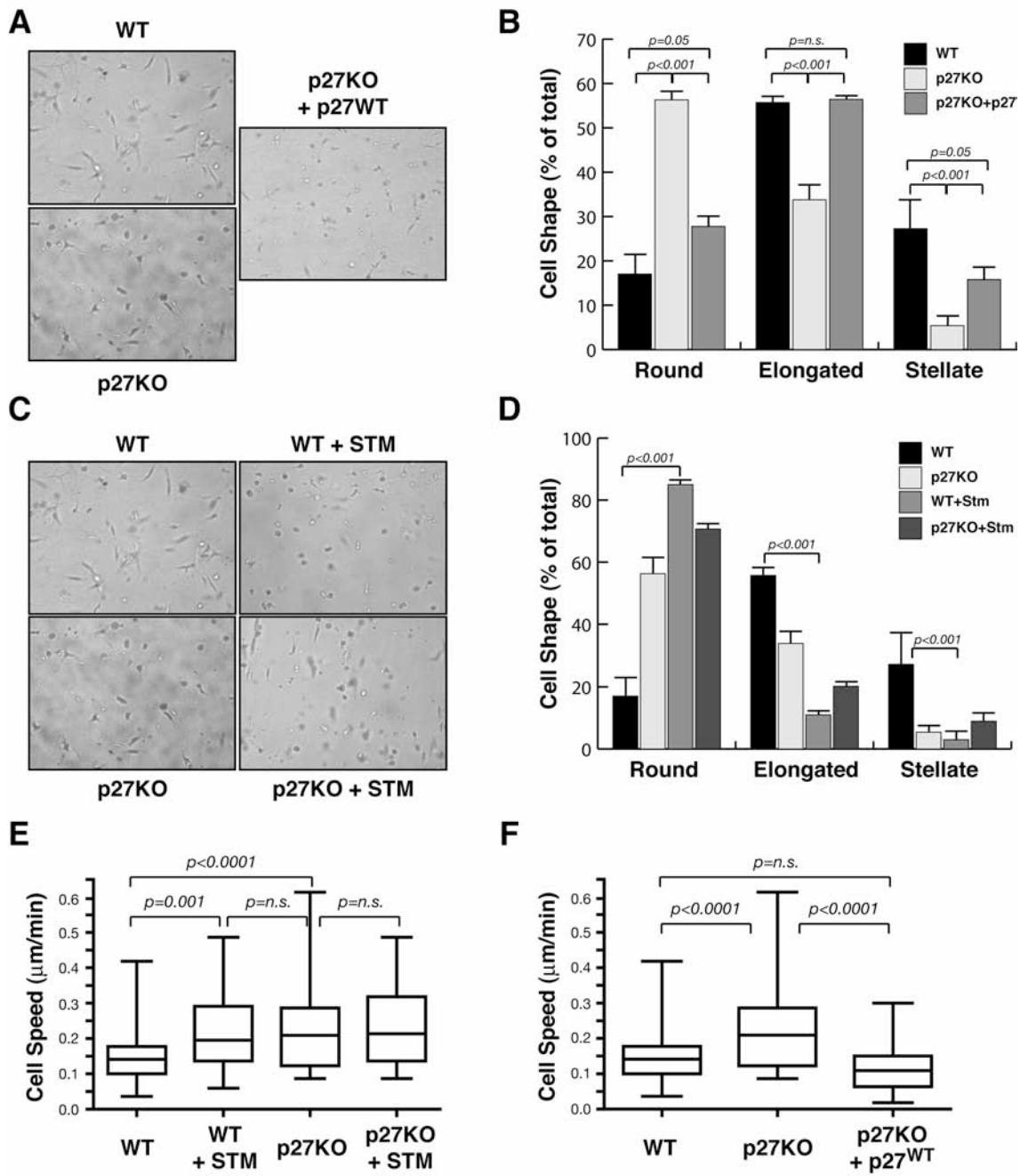
of nocodazole prevents protrusion formation and considerably increases cell motility of WT cells immersed in 3D-Collagen I. **Video S4** shows the time dependent internalization of lipid rafts in WT fibroblasts. **Video S5** shows that the time dependent internalization of lipid rafts in p27 KO fibroblasts is faster than in WT cells. **Video S6** shows that the faster internalization of lipid rafts of p27 KO fibroblasts relies on the decreased MT stability of these cells, since it is abolished by Taxol treatment. **Video S7** shows that p27 KO cells immersed in 3D-Collagen I remain rounded and move with an amoeboid-like motility. **Video S8** shows that p27 KO cells treated with Dynasore form protrusion and fail to move. **Video S9** shows that p27 KO cells transfected with the Control-Sh vector immersed in 3D-Collagen I remain rounded and move with an amoeboid-like motility. **Video S10** shows that p27 KO cells transfected with the Caveolin 1-Sh vector immersed in 3D-Collagen I form protrusion and fail to move.

A**B****C**

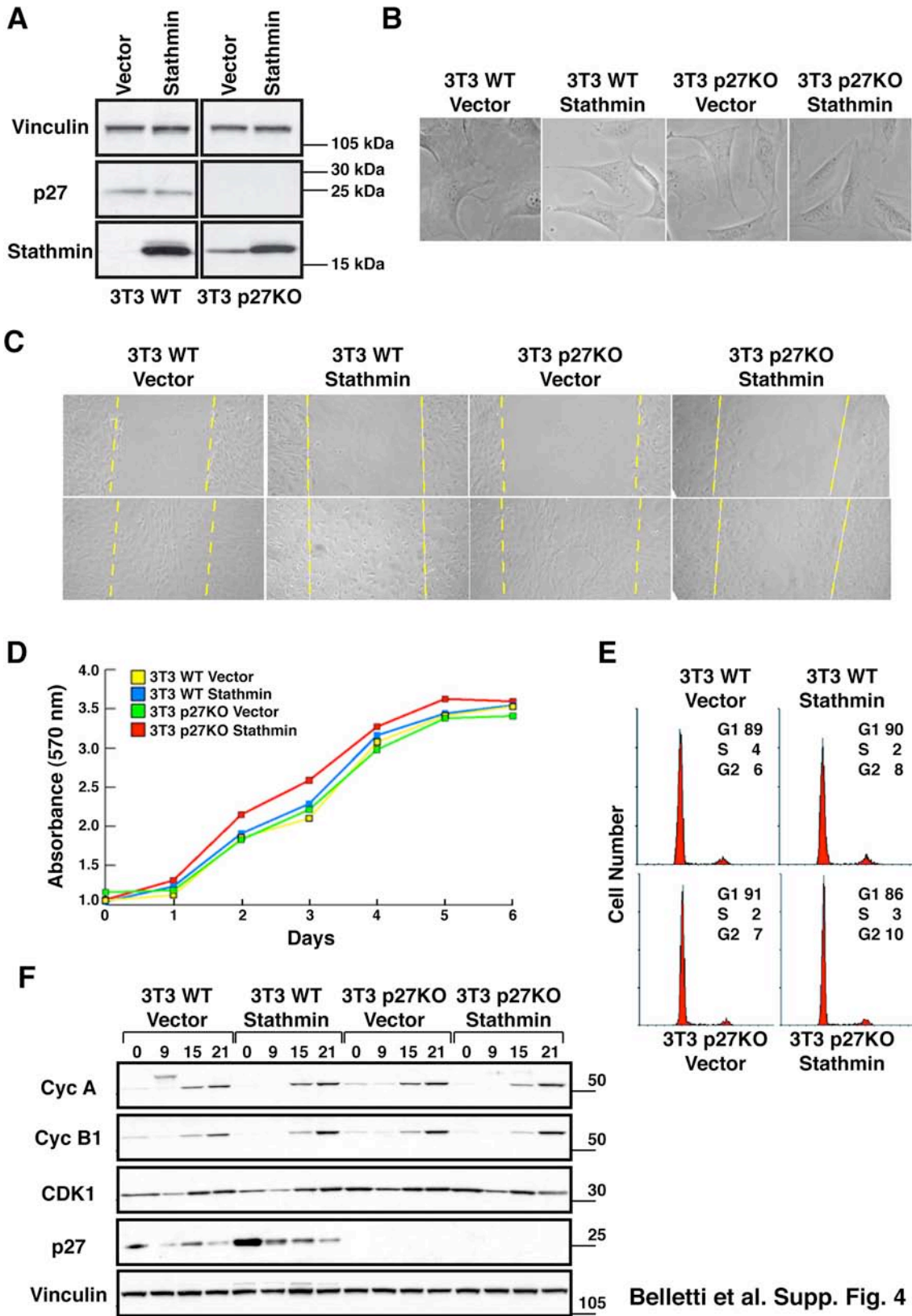
Belletti et al. Supp Fig.1

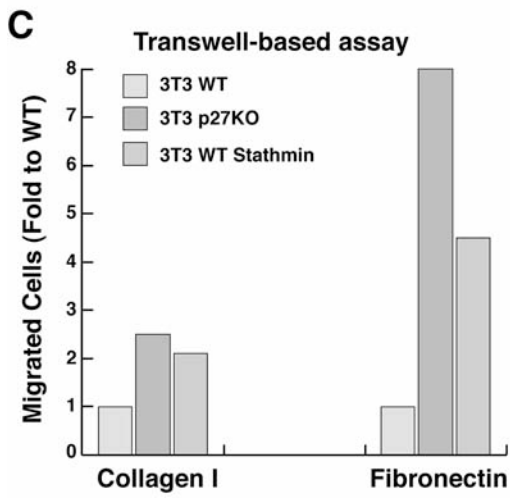
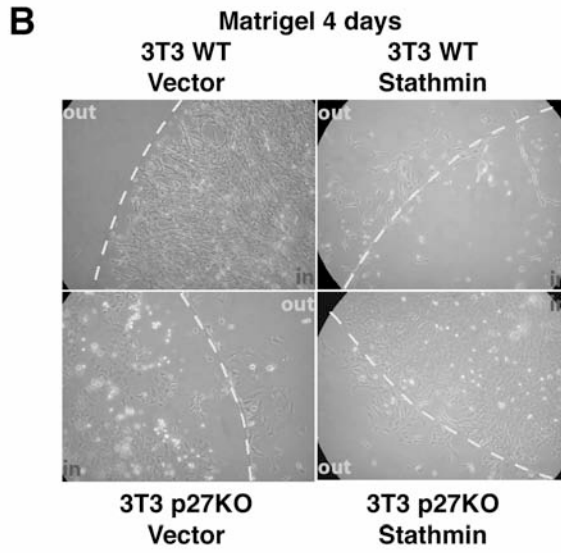
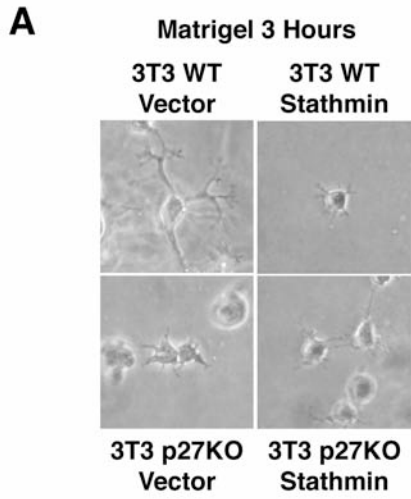


Belletti et al. Supp. Fig. 2

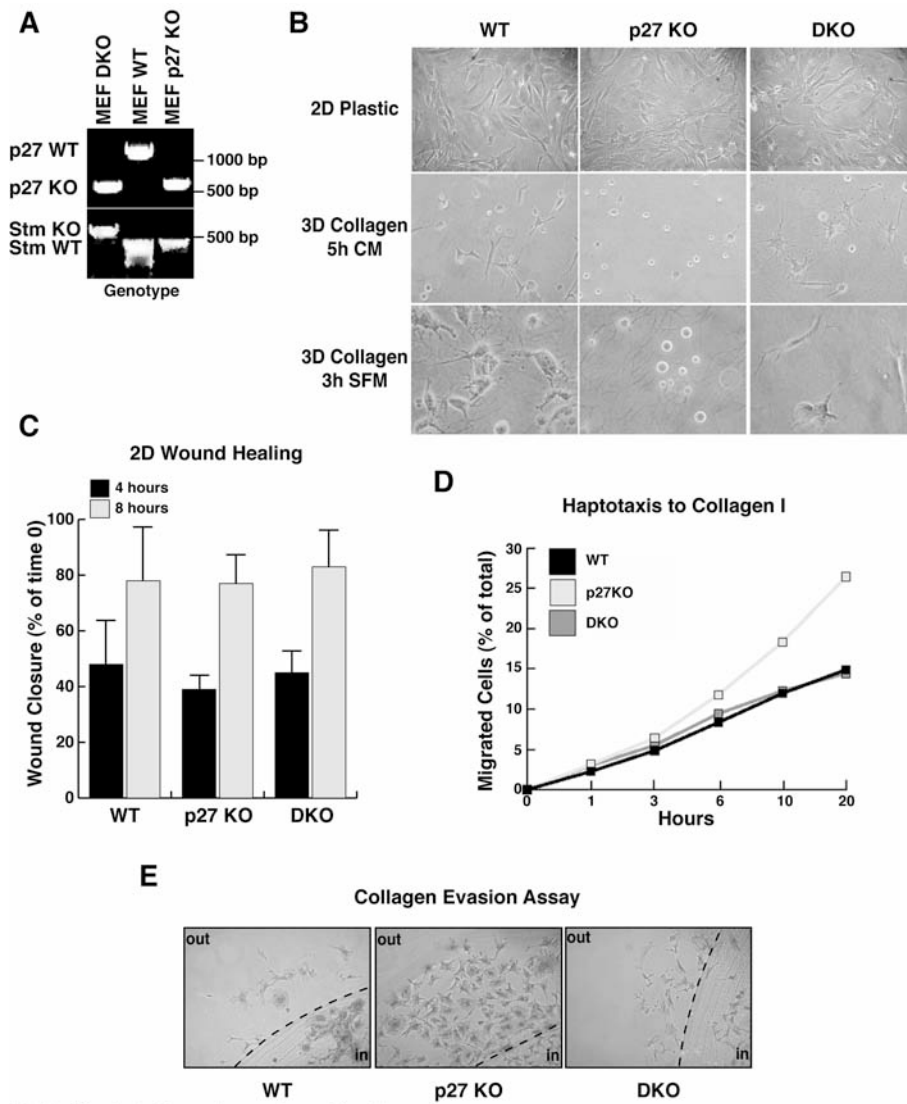


Belletti et al. Supplementary Fig. 3

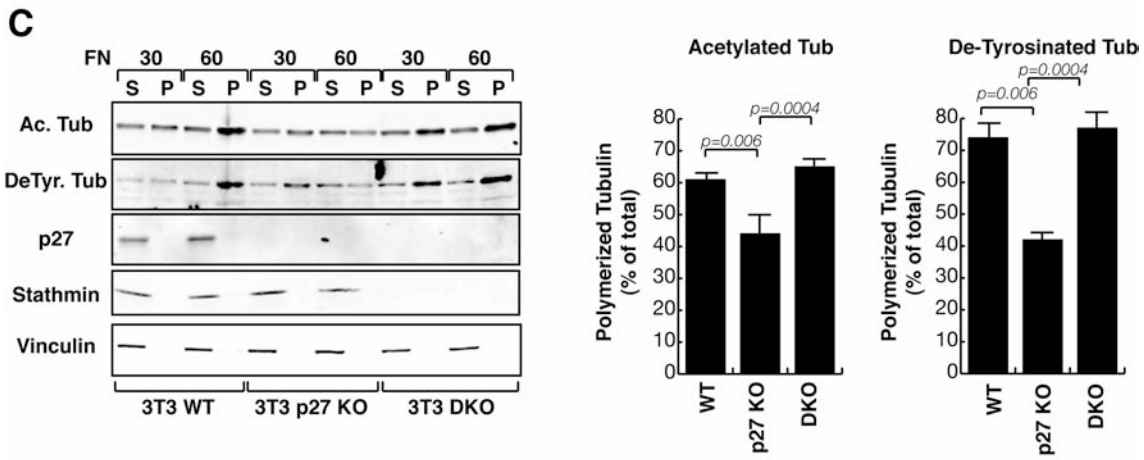
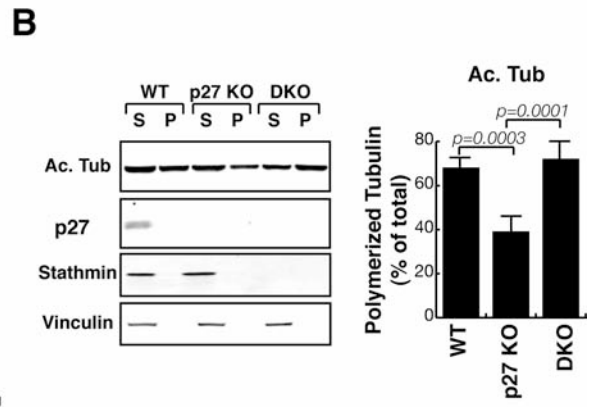
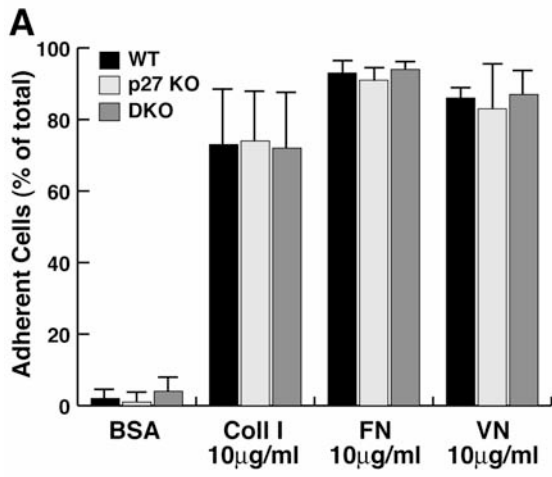




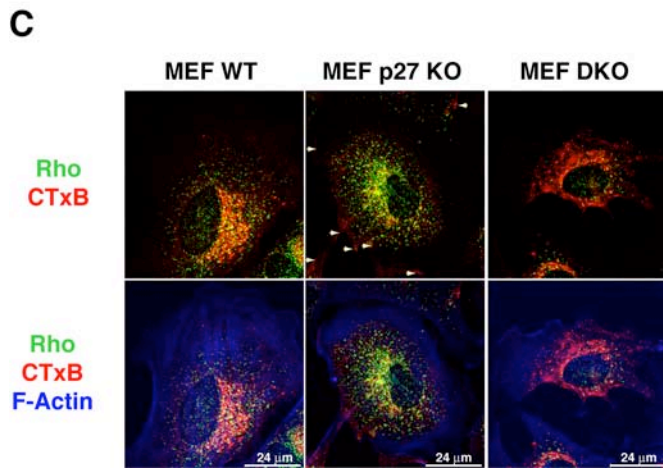
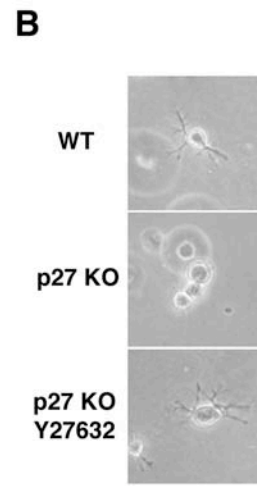
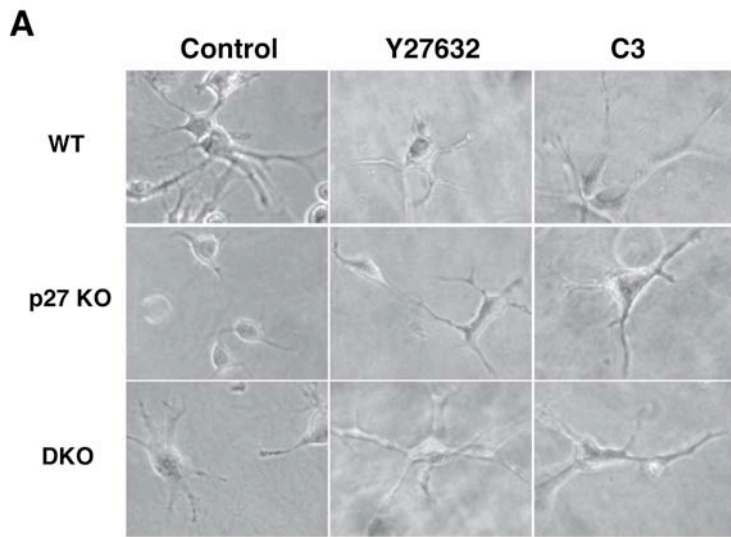
Belletti et al. Supp. Fig. 5



Belletti et al. Supplementary Fig. 6



Belletti et al. Supp. Fig. 7



Belletti et al. Supp. Fig. 8